

Construction of m6a-Related lncRNA Signature to Predict Aggressiveness, M6a Modification Level, and Drug Resistance of Hepatocellular Carcinoma

Bobin Ning^{1*}, Xueguo Wang², Dongming Li² and Lu Lu²

¹Department of General Surgery, Chinese PLA General Hospital, Beijing, People's Republic of China, Haidian, Beijing, China

²Department of Hepatobiliary and Pancreatic Surgery, The Second Affiliated Hospital of Hainan, Longhua, HaiKou, China

*Corresponding author: Bobin Ning, Department of General Surgery, Chinese PLA General Hospital, Beijing, People's Republic of China, Haidian, Beijing, China, Tel: 15140239706; E-mail: 15140239706@163.com

Received date: December 09, 2021; Accepted date: December 23, 2021; Published date: December 30, 2021

Citation: Ning B, Wang X, Li D, Lu L (2021) Construction of m6a-Related lncRNA Signature to Predict Aggressiveness, M6a Modification Level, and Drug Resistance of Hepatocellular Carcinoma. J Infect Dis Ther 9: 483.

Copyright: © 2021 Ning B, et al. This is an open-access article distributed under the terms of the Creative Commons Attribution License, which permits unrestricted use, distribution, and reproduction in any medium, provided the original author and source are credited.

Abstract

Backgrounds: Hepatocellular Carcinoma (HCC) is the fourth-ranked malignant tumor with only 18% of 5-year Overall Survival (OS). Currently, the means of invasive detection for HCC patients are still inadequate. M6a methylation has been demonstrated to contribute to tumorigenesis and progression through the regulation of ncRNAs. Therefore, the construction of an asynchronous prediction pattern by m6A-lncRNA regardless of the expressed level is meaningful for HCC patients' diagnosis and potential mechanism study.

Methods: We initially identified m6A-lncRNAs through Pearson correlation coefficients. After screening differential m6A-lncRNAs between the cancerous and paracancerous tissues, the lncRNA pairs were formed for further univariate analysis. Incorporate multi-clinical information, we determined 10 pairs of m6A-lncRNA into the prediction model by lasso regression analysis. Next, we determined the optimal cut-off value to distinguish high- and low-risk groups in HCC patients. Finally, we validated the model in terms of survival, clinicopathological characteristics, m6a genes, Tumor Microenvironment (TME), and chemotherapy.

Results: Compared with clinical traits such as age, grades, and stages, the model composed of 10 pairs of DEm6A-lncRNA had a better prediction of HCC prognosis in patients. Moreover, it can serve as a risk factor for independent prognosis of HCC patients' survival status (HR=1.38, p<0.001). Aggressive clinic-pathological characteristics, TME, differences of m6A-regulators, and chemotherapeutics sensitivity were also predictable and separable according to the pair-model.

Conclusion: The research suggests m6a-lncRNA pair-model is critical clinical meaningfulness for clinical prognosis and pathological characteristics, to the TME, and chemotherapeutic effect in HCC.

Keywords: LIHC; lncRNA signature; m6a methylation modification; Prognosis

Introduction

Hepatocellular Carcinoma (HCC) is the leading cause of cancer-related deaths across the world. Over the past decades, substantial progress has been achieved in understanding of epidemiology, hazard factors, and molecular characteristics of HCC [1]. However, most patients are difficult to be detected at the early stage and have a poor prognosis with a high recurrence rate at 5 years after surgery. Given the fact that surgery and other interventions are very traumatic, especially for middle-aged or even elder patients, who are relatively unfit to tolerate such procedures, identifying therapeutic and prognostic targets for HCC could significantly benefit more HCC patients. Nowadays, more than 100 kinds of RNA modifications have been demonstrated, among which m6A methylation modification is the most widely studied. An extensive series of studies have shown that m6A methylation has a strong contribution to the development of various tumors. Among the 163 recognized types of RNA chemical modifications, m6A is considered to be the most prevalent, abundant, and conserved mode for eukaryotic messenger RNAs (mRNAs),

miRNAs, and lncRNAs, and impacts those RNAs in multiple aspects including transcription, processing, translation and metabolism [2-6].

The m6A methylation modification involves the methylation of the N atom at the 6th position of Adenine (A) in RNA and this biological process mainly participates by three enzymes, namely methyltransferases, demethylases, and methylation recognition enzymes. Methyltransferases include METTL3, METTL14, METTL16, WTAP and KIAA1429, RBM15/15B [7]. The first identified methyltransferase-METTL3, has been demonstrated to participate in lipid metabolism and circadian rhythm. m6A methylation is dynamic and reversible, and the process is regulated by demethylation enzymes-FTO, ALKBH5, etc. regulated. YTHDC12, YTHDF123, HNRNPA2B1, eIF3, which specifically bind to the m6A methylation region and contribute to the regulation of RNA structure [8].

Long chain non-coding RNAs (lncRNAs) are non-coding RNAs longer than 200nt[9]. They do not encode proteins and are involved in various physiological and pathological activities in the human body by

regulating gene expression [10]. Several studies have shown that m6A methylation modifications exert regulatory effects by altering the structure of lncRNAs [9]. M6A methylation modifications can participate in the transcriptional silencing of genes on chromosome X by regulating the lncRNA X-Inactive Specific Transcript (XIST). M6A methylation modifications consist of at least 78 methylated sites on XIST, and knockdown of methyltransferases METLL13 or RBM15 /15B can affect gene expression on the X chromosome. YTHDC1 preferentially recognizes methylation sites on XIST, which in turn induces XIST-mediated gene silencing, while YTHDF2 is involved in the functional expression of Dendritic Cells (DCs) through the regulation of lnc-Dpf3 [10].

Previous studies have shown that lncRNA expression patterns can induce tumorigenesis as well as biological processes-tumor proliferation, invasion, and metastasis. The study of m6A-lncRNA in tumors is still at the preliminary stage. The relevant regulation mechanisms are still unclear which need further research and exploration. In this study, we intend to develop an m6A-lncRNA pairs signature for HCC patients and demonstrate the correlation between m6A methylation and prognosis, tumor microenvironment, and chemotherapy sensitivity of HCC patients [11].

Methods

Retrieval of transcriptome data, preparation, and differentially expressed analysis

HCC transcriptome analysis (RNAseq) data along with patient clinical data were downloaded from TCGA. GTF files were downloaded from Ensembl for annotation to separate mRNAs and lncRNAs [12]. A list of recognized m6a regulators was obtained from the previous studies. Pearson analysis was performed by using the R package limma to identify m6a methylation-associated lncRNAs. The filter criteria were set as Pearson correlation coefficient $|\geq 0.4$ and P value ≤ 0.001 .

Construction of differentially expressed m6a-lncRNA pairs

We screened DEM6a-lncRNAs through the differentially expressed analysis between normal and HCC tissues. $\log_{2}FC > 1$ as well as $FDR < 0.05$ was considered as statistical. Then the DEM6a-lncRNAs were cyclically paired with each other. Assuming that X is the value of the lncRNA pairs matrix constructed by lncRNA A and lncRNA B, X is defined as 1 if the expression level of lncRNA A is higher than lncRNA B, otherwise, X is defined as 0. Then, the DEM6a-lncRNA pairs are constructed into a 0-1 matrix. However, a valid match was deemed when the number of lncRNA pairs with the expression of 0 or 1 accounted for more than 20% of the total [13-15].

Establishment of lncRNA-pairs model

Next, we conducted a univariate survival analysis on DEM6a-lncRNA pairs by R package survivor. P value < 0.05 was identified as prognostically relevant. Then, we performed cross-validation by Lasso regression analysis using the "Glmnet" package to downscaling of DEM6a-lncRNA pairs and constructed a prognosis-related risk assessment model. To verify the accuracy of the constructed model, we further constructed ROC curves for 1, 3 and 5 years; the AUC values of this model were simultaneously calculated. Considering the sensitivity and specificity of the diagnostic criteria, the best cut-off

point was certificated to distinguish the high-risk and low-risk groups of HCC patients [16-18].

Validation of the constructed lncRNA-pairs model

To validate the accuracy and feasibility of the risk model, the specific risk scores and survival status of each sample in the model were also visualized. Kaplan-Meier analysis was also performed for the HCC patients from the TCGA database, and the difference of survival between the high- and low-risk groups was visualized by the "survival" package. Furthermore, we discovered the clinical application of the risk model, a chi-square test was performed to analyze the clinic pathological characteristics between the high- and low-risk groups. Band plots were applied for visualization and are labeled as follows, $< 0.001 = ***$, $< 0.01 = ****$, and $< 0.05 = *$.

Wilcoxon signed rank test was used to calculate the variation of risk scores among the subtypes for different clinicopathological characteristics. To confirm whether the model could be used as an independent predictor of clinical prognosis, univariate and multivariate Cox regression analyses were performed among the risk scores and clinicopathological characteristics. The R packages survival, pHeatmap, and ggpubr were utilized in the above operations.

Investigation of tumor-infiltrating immune cells and analyses of the m6a methylation modification related molecules

Aiming to reveal the potential interactions between lncRNA pairs and tumor microenvironment, we performed the lncRNA-pairs score-based calculation of immune microenvironment by six different computational methods, including XCELL, TIMER, QUANTISEQ, MCPOUNTER, CIBERSORT-ABS, and CIBERSORT. Wilcoxon signed-rank test was also conducted to validate the differences of immune infiltration between high- and low- risk groups. By Spearman correlation analysis, we further demonstrated the relationship between lncRNA-pair score and immunocyte infiltration by box plots with the significance threshold set at $P < 0.05$. The above arithmetic procedure was implemented by R packages limma, scales, ggplot2 and ggtext. To explore the m6A regulators, we exhibited the m6a expression between the risk subgroups [19].

Exploration of the significance of the model in the clinical treatment

To determine whether the model can be used to guide clinical chemotherapy regimens, we calculated the commonly used antitumor drugs - Cisplatin, Gemcitabine, Lapatinib and Mitomycin - in clinical HCC patients. Base on the TCGA project, wilcoxon test was conducted to compare the IC50 of the above chemotherapy drugs to assess the sensitivity between the lncRNA-pair subgroups. The algorithm was implemented by the R package pRRophetic and ggplot2. P-values < 0.05 were considered statistically significant [20].

Results

Identification of differentially expressed m6a-lncRNAs in LIHC

The workflow of this study is exhibited in Figure 1. First, we downloaded transcriptomic data and clinical information from the

TCGA database, including 50 normal samples and 374 tumor samples. After dividing the expression profiles into mRNA and lncRNA matrices, m6a regulators expression profiles were constructed. Co-expression analysis was performed to obtain the m6a-lncRNAs. A total of 127 DEM6a-lncRNAs (Figure 2A) were screened in LIHC patients which were all over-expressed in tumor tissues (Figure 2B).

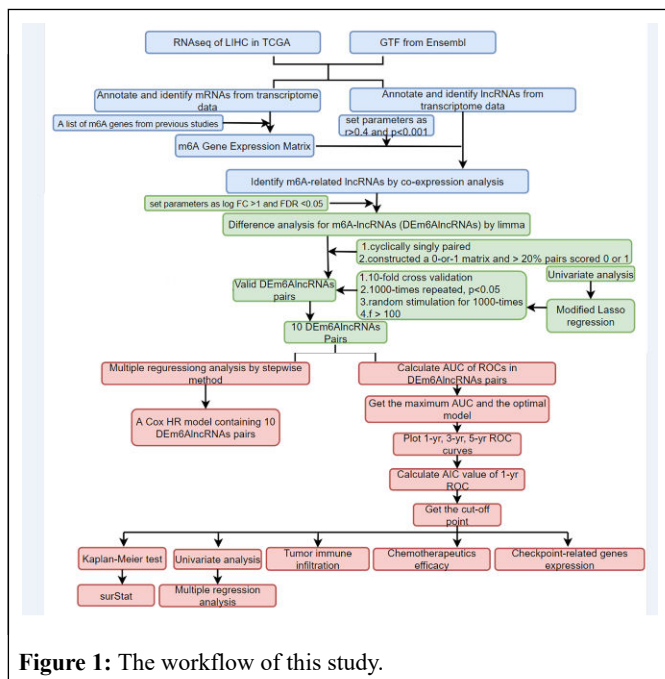


Figure 1: The workflow of this study.

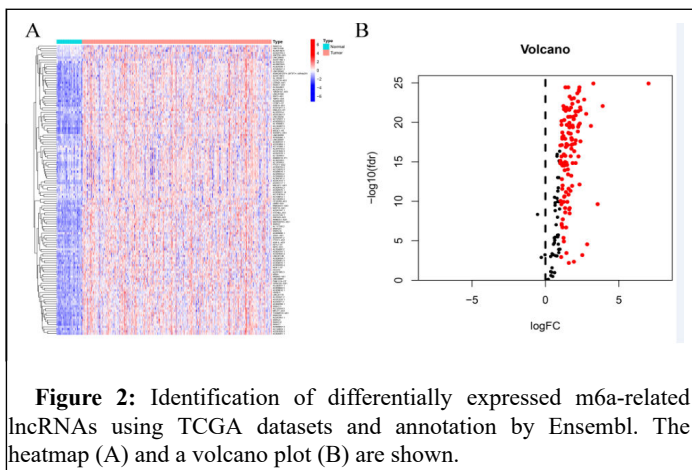


Figure 2: Identification of differentially expressed m6a-related lncRNAs using TCGA datasets and annotation by Ensembl. The heatmap (A) and a volcano plot (B) are shown.

Establishment of DElncRNA pairs and a risk assessment model

127 DEM6a-lncRNAs were enlisted to construct 0-1 matrix, and then univariate survival analysis and Lasso regression analysis were conducted to formate lncRNA-pair models (Figure 3A, 3B), and then we performed univariate and multivariate Cox analysis on these 10 pairs of DE-m6alncRNA pairs to determine their ability as an independent clinical prognostic factor (Figure 3C, 3D) [21].

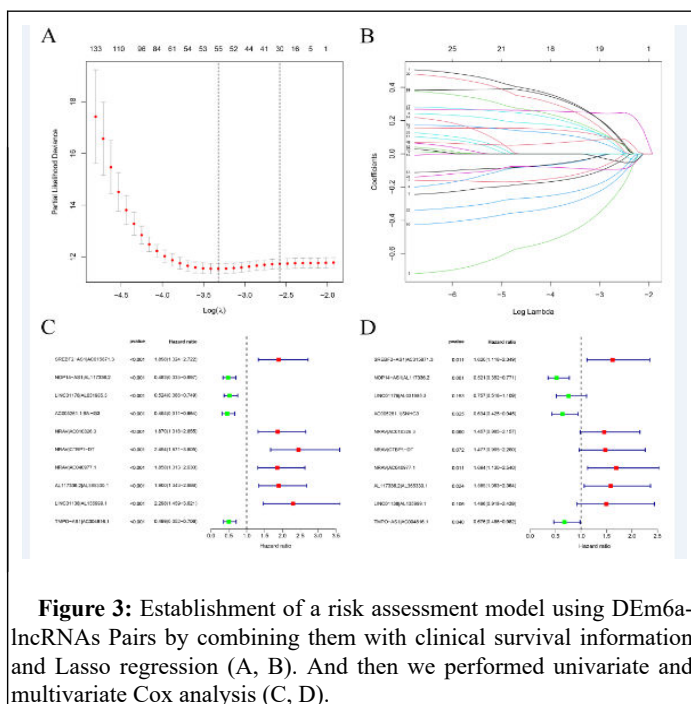


Figure 3: Establishment of a risk assessment model using DEM6a-lncRNAs Pairs by combining them with clinical survival information and Lasso regression (A, B). And then we performed univariate and multivariate Cox analysis (C, D).

Clinical evaluation by risk assessment model

Next, we plotted the 1-year ROC curve and calculated the area under the curve (AUC) of 0.772, which means the lncRNA-pair model can reflect the overall survival of HCC patients accurately (Figure 4A). As the ROC curves shown in Figure 4B, we confirm the optimal cut-off value at 1.1612. To further detect the accuracy and stability of our model, we also plotted the ROC curves for 3 and 5 years in which all the AUC values exceeded 0.7 (Figure 4C). We respectively measured the AUC values of lncRNA pairs against each clinical index (age, gender, tumor grade, and T) and presented them uniformly in Figure 4D. The results reflected that the AUC value of the lncRNA-pair model substantially exceeded other parameters [22].

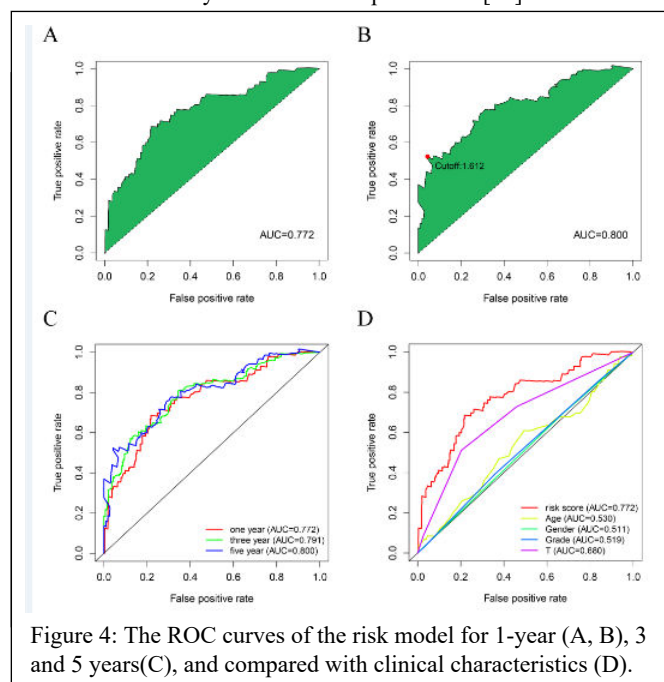


Figure 4: The ROC curves of the risk model for 1-year (A, B), 3 and 5 years(C), and compared with clinical characteristics (D).

Based on the optimal cut-off value, we divided the HCC patients into high-risk and low-risk groups.

Risk scores and survival status for each case are displayed in Figure 5A, 5B. Kaplan-Meier analysis between the two subgroups is shown in Figure 5C ($p < 0.001$), which presents that the low-risk group has significantly better outcomes than the high-risk group [23].

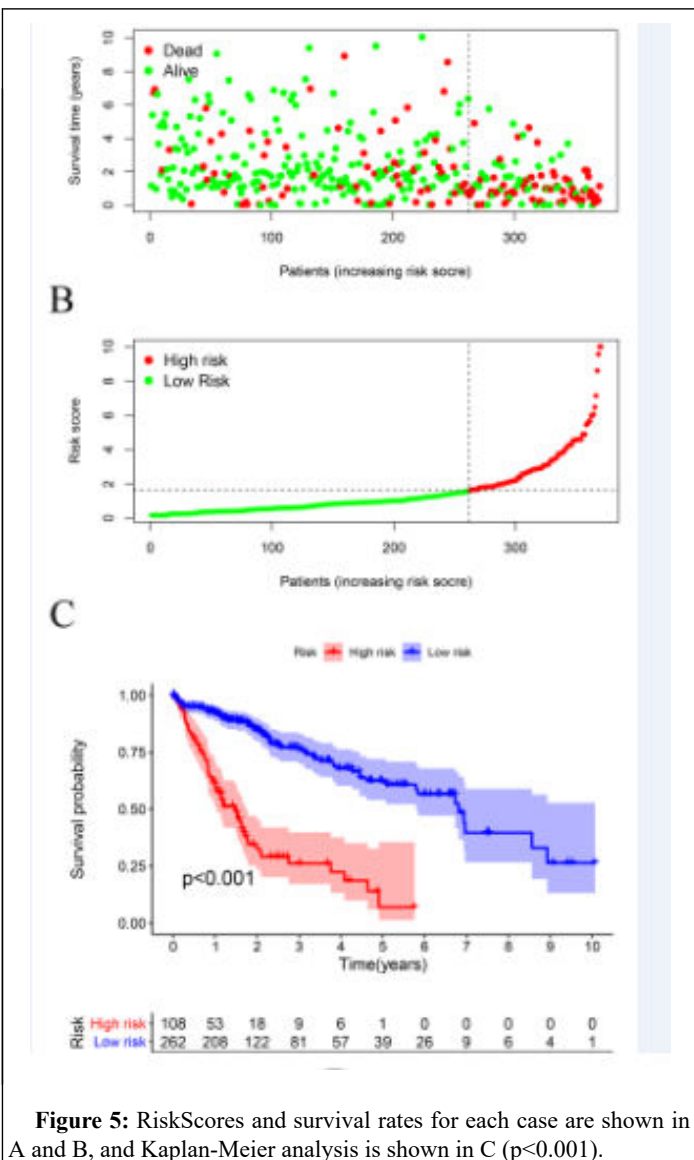


Figure 5: RiskScores and survival rates for each case are shown in A and B, and Kaplan-Meier analysis is shown in C ($p < 0.001$).

Then a series of chi-square tests were conducted to investigate the relationship between LIHC risk and clinicopathologic characteristics. The bar chart (Figure 6A) and corresponding scatter plot obtained by Wilcoxon signed rank test showed that T-stage (Figure 6B), tumor grade (Figure 6C) and clinical stage (Figure 6D) were significantly associated with risk. Next, we showed by univariate Cox regression analysis (Figure 6E) that T-stage ($P < 0.001$, HR=1.688, 95% CI [1.407-2.026]) and riskScore ($P < 0.001$, HR=1.338, 95% CI [1.264-1.417]) showed statistical differences. Multivariate Cox regression analysis also showed that the above indications could be used as independent prognostic predictors for patients with LIHC (Figure 6F).

In conclusion, the m6a-lncRNA-based risk assessment model can be used not only as a reliable predictor of survival outcome but also as a reliable indicator of tumor growth in patients with LIHC.

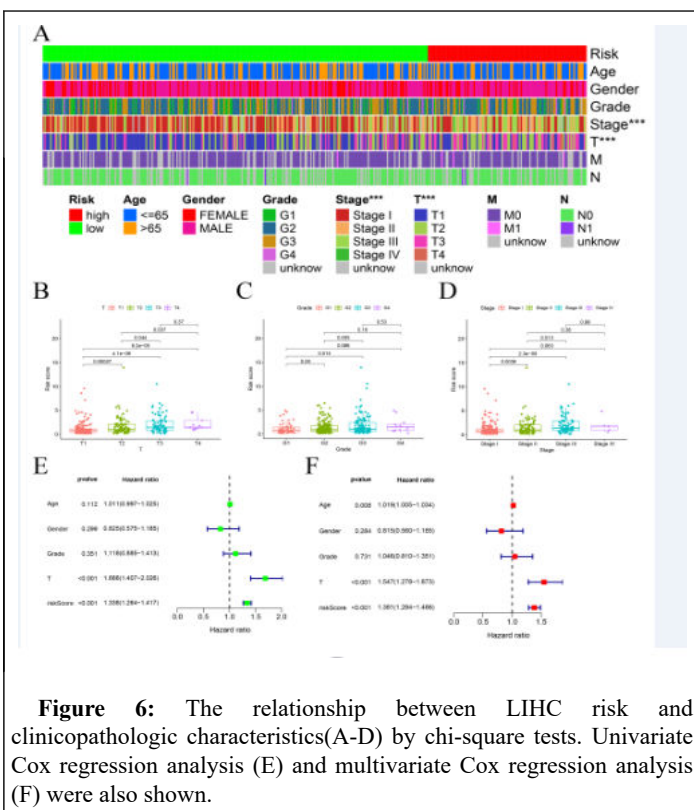


Figure 6: The relationship between LIHC risk and clinicopathologic characteristics(A-D) by chi-square tests. Univariate Cox regression analysis (E) and multivariate Cox regression analysis (F) were also shown.

Assessment of the risk model with tumor immune microenvironment, and the m6a related genes

To investigate whether the model reflects tumor-infiltrating immune cells in LIHC, we performed correlation analysis of immune cells by seven different software, and the results of different software will be shown in different colors (Figure 7). B-cells, T-cell CD4+ memory, NK cells, T-cell CD4+ Th2, myeloid dendritic cells, monocytes, T-cell CD8+, macrophages, Tregs, mast cell quiescence, and macrophage M0 were positively correlated with risk values in the model; T cell CD4+ memory quiescence, macrophage M1, endothelial cells, hematopoietic stem cells, mesenchymal cells, mast cell activation, and neutrophils were negatively correlated. We then counted immune cell infiltration in LIHC patients in both high- and low-risk groups and the results were shown in Figure 8A-Z, where endothelial cells, hematopoietic stem cells, macrophage cells, monocyte cells, neutrophil cells, stroma score, T cell CD4+, T cell CD8+ were significantly different between the subgroups ($P < 0.0001$).

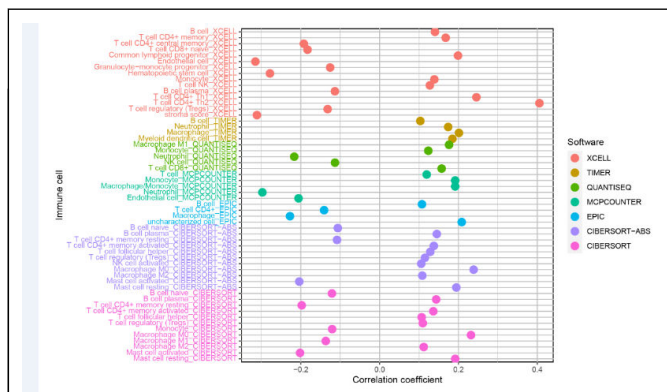


Figure 7: The correlation analysis of immune cells by seven different software.

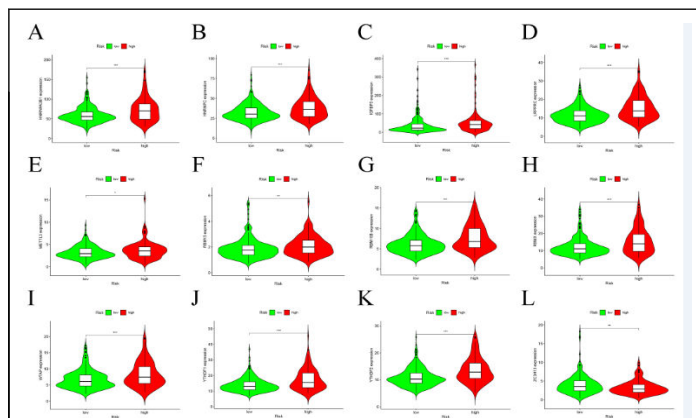


Figure 9: The differential expression of m6a methylation modification-related genes between the two groups (A-L).

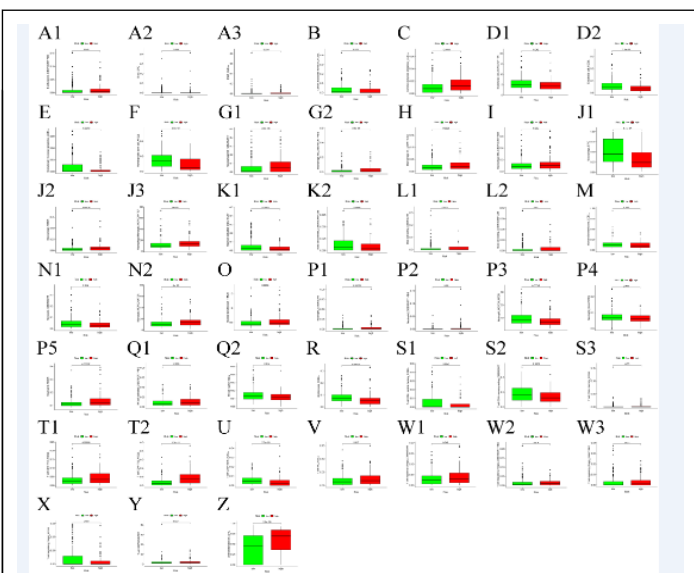


Figure 8: The immune cell infiltration in LIHC patients in both high- and low-risk groups (A-Z).

To further investigate whether this risk model is associated with m6a methylation modification-related genes, we counted the distribution of differential expression characteristics of m6a methylation modification-related genes between the two groups. Our observations showed (Figure 9A-L) that HNRNPA2B1, IGFBP3, LRPPRC, METTL3, WTAP, YTHDF1, YTHDF2, ZC3H13, HNRNPCs, RBM15, RBM15B, RBMX were significantly different between the two groups ($P < 0.05$).

Analysis of the correlation between the risk model and chemotherapeutics

Finally, we tried to validate the association between the risk model and the efficacy of common chemotherapeutic drugs used to treat LIHC. We determined the correlation between our risk model and drug sensitivity in patients with liver cancer by analyzing the IC50 of different drugs between high and low risk groups. We validated a total of four chemotherapeutic agents commonly used in the clinic for hepatocellular carcinoma, namely Cisplatin, Gemcitabine, Lapatinib and Mitomycin (Figure 10A-D). The results showed that higher risk scores were all associated with lower IC50 ($P < 0.01$) in Cisplatin, Gemcitabine and Mitomycin, indicating that our risk model can be used to effectively predict the outcome of chemotherapy in patients with hepatocellular carcinoma [24].

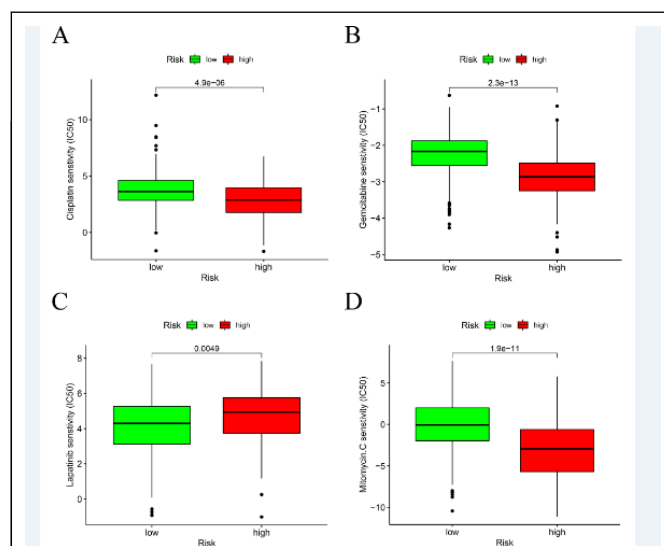


Figure 10: The correlation between our risk model and drug sensitivity by analyzing the IC50 of different drugs between high- and low-risk groups (A-D).

Discussion

Since the development of second-generation sequencing technology, the role of m6A methylation modification in tumorigenesis has become a hot topic of research. Considerable investigations have demonstrated that m6A methylation can participate in various life activities such as lipid metabolism, gene expression, and immune response, especially in tumorigenesis, metastasis, and drug resistance. The differential expression of m6A methyltransferase and recognition proteins was found in several tumors including HCC, while the abundance of m6A regulators in HCC was also found to be extremely abnormal compared to normal tissues [25]. These anomalies suggest that m6A regulators may contribute to extraordinary expression or dysfunction of oncogenes. For example, lncRNA has been identified to play an important role in tumor progression, and the m6A level of lncRNA may affect its sponge miRNA function, nucleation, and degradation. ZUO X has been found that m6A regulators mediate the upregulation of lncRNA00958 which can affect lipid metabolism in HCC and promote HCC progression.

A large number of studies have been devoted to building models based on lncRNA expression levels to predict the prognosis of cancer patients [18, 19], most of which are based on quantitative comparisons of transcript expression levels. However, few studies have explored predicting the prognostic outcome of patients with malignancies by analyzing m6A-lncRNA pairings. In this study, instead of assessing the specific expression values of individual lncRNAs, we attempted to construct a reasonable risk prediction model using two m6A-lncRNA pairing combinations that did not require exact measurement of their specific expression levels in the study. Thus, this novel model has the advantage of feasibility and generalizability to clinical practice in different patients. Furthermore, we calculated the AIC value to find the best cut-off point to classify patients into high- and low-risk groups. Based on the group assessment of our risk model, the prognosis of patients in the high-risk group was significantly worse than that in the low-risk group. The T-stage was significantly higher in the high-risk group. This indicates that our model is highly efficient and specific for determining proliferation and differentiation ability. Deeper biological information mining is performed to evaluate the risk assessment model with survival outcomes, clinical characteristics, tumor microenvironment components, m6a regulators, and chemotherapy sensitivity. This implies a reliable performance of the modeling algorithm [26].

Previous studies have demonstrated that m6A methylated genes can be involved in tumor growth and metastasis by modifying lncRNAs. The lncRNA MALAT-1 is the first long-stranded non-coding RNA identified to be associated with lung cancer. There exists a triple helix structure at its 3' end, and the deletion or mutation of this structure can affect the stability and functional expression of MALAT1. METTL16, a methyltransferase, can bind to the triple helix structure at the 3' end of lncRNA MALAT1 to affect its structural stability and functional expression, thus participating in tumor development. The lncRNA GAS5-YAP-YTHDF3 axis involves significantly contributing to Colorectal Cancer (CRC) invasion and metastasis. lncRNA GAS5 can directly combine with YAP and promote its phosphorylation and degradation, while YAP can target YTHDF3 and positively correlate with its expression. In turn, YTHDF3 can promote the degradation of GAS5 through m6A methylation. Knockdown of YTHDF3 dramatically extends the rate of GAS5 degradation and reduces the expression of YAP protein. Therefore, YTHDF3 could be involved in regulating the invasion and metastasis of CRC through regulating the

degradation of GAS5. Although several studies have partially demonstrated that m6A methylation modifications can engage in tumor progression in the form of the modulation of lncRNAs, but whether they are involved in tumor drug resistance has not been reported yet. However, our risk model assessment also demonstrated that the classical m6a regulators were remarkably elevated in the high-risk group, suggesting that the level of m6a methylation modifications was enhanced in the high-risk group. This is in full agreement with the results predicted in our present study. Other than that, our study also pioneered the relationship between changes in m6A-lncRNA levels and the tumor microenvironment of HCC and chemotherapy sensitivity in HCC patients. This could provide a new target and theoretical basis for future therapeutic targets for HCC patients.

The study also has some drawbacks and limitations. For example, the risk assessment model was constructed entirely based on the original dataset of TCGA, but it was not validated with additional HCC patient cohorts, which still needs further validation and exploration by basic experiments and clinical data.

Conclusion

In summary, this study constructed a risk signature based on 10 pairs of m6 m6AlncRNA pairs for HCC. The risk model can not only serve as an independent clinical prognostic factor for HCC patients but also accurately detect clinical characteristics - tumor T-stage, grade and clinical stage. For further in-depth biological perspectives, those m6A-lncRNA pairs were tumor microenvironment, m6a regulators, and chemotherapy sensitivity. This hyper-sensitive and indicative hazard signature provides an innovative theoretical basis for predicting the biological characteristics of HCC and improving clinically guided treatment options.

Disclosure of interest

The authors declare no conflict of interest.

References

1. Carr BI, Guerra V, Donghia R, Yilmaz S (2020) Trends in tumor indices in relation to increased hepatocellular carcinoma size: Evidence for tumor evolution as a function of growth. *J Gastrointest Cancer* 51: 1215-1219.
2. Shen F (2015) Research progress in improving the efficacy of surgical treatment of primary liver cancer. *Zhonghua Zhong Liu Za Zhi* 37: 643-646.
3. Desrosiers R, Friderici K, Rottman F (1974) Identification of methylated nucleosides in messenger RNA from Novikoff hepatoma cells. *Proc Natl Acad Sci U S A* 71: 3971-3975.
4. Roundtree IA, Evans ME, Pan T, He C (2017) Dynamic RNA modifications in gene expression regulation. *Cell* 169: 1187-1200.
5. Wang X, Zhao BS, Roundtree IA, Lu Z, Han D, et al. (2015) N(6)-methyladenosine modulates messenger rna translation efficiency. *Cell* 161: 1388-1399.
6. Chen XY, Zhang J, Zhu JS (2019) The role of m(6)A RNA methylation in human cancer. *Mol Cancer* 18: 103.
7. Zhong X, Yu J, Frazier K, Weng X, Li Y, et al. (2018) circadian clock regulation of hepatic lipid metabolism by modulation of m(6)A mRNA methylation. *Cell Rep* 25: 1816-1828.e4.
8. Robinson M, Shah P, Cui YH, He YY (2019) The role of dynamic m(6) a rna methylation in photobiology. *Photochem Photobiol* 95: 95-104.

9. Ai B, Kong X, Wang X, Zhang K, Yang X, et al. (2019) LINC01355 suppresses breast cancer growth through FOXO3-mediated transcriptional repression of CCND1. *Cell Death Dis* 10: 502.
10. Chen Z, Tao Q, Qiao B, Zhang L (2019) Silencing of LINC01116 suppresses the development of oral squamous cell carcinoma by up-regulating microRNA-136 to inhibit FN1. *Cancer Manag Res* 11: 6043-6059.
11. Patil DP, Chen CK, Pickering BF, Chow A, Jackson C, et al. (2016) m(6)A RNA methylation promotes XIST-mediated transcriptional repression. *Nature* 537: 369-373.
12. Liu J, Zhang X, Chen K, Cheng Y, Liu S, et al. (2019) CCR7 Chemokine receptor-inducible lnc-Dpf3 restrains dendritic cell migration by inhibiting HIF-1 α -mediated glycolysis. *Immunity* 50: 600-615.e15.
13. Qiu JJ, Wang Y, Liu YL, Zhang Y, Ding JX, et al. (2016) The long non-coding RNA ANRIL promotes proliferation and cell cycle progression and inhibits apoptosis and senescence in epithelial ovarian cancer. *Oncotarget* 7: 32478-92.
14. Visvanathan A, Patil V, Abdulla S, Hoheisel JD, Somasundaram K, et al. (2019) N(6)-methyladenosine landscape of glioma stem-like cells: METTL3 is essential for the expression of actively transcribed genes and sustenance of the oncogenic signaling. *Genes (Basel)* 10(2): 141.
15. Klinge CM, Piell KM, Tooley CS, Rouchka EC (2019) HNRNPA2/B1 is upregulated in endocrine-resistant LCC9 breast cancer cells and alters the miRNA transcriptome when overexpressed in MCF-7 cells. *Sci Rep* 9: 9430.
16. Yang Z, Li J, Feng G, Gao S, Wang Y, et al. (2017) MicroRNA-145 modulates N6-methyladenosine levels by targeting the 3'-untranslated mRNA region of the N6-methyladenosine binding YTH domain family 2 protein. *J Biol Chem* 292: 3614-3623.
17. Zuo X, Chen Z, Gao W, Zhang Y, Wang J, et al. (2020) M6A-mediated upregulation of LINC00958 increases lipogenesis and acts as a nanotherapeutic target in hepatocellular carcinoma. *J Hematol Oncol* 13.
18. Hong W, Liang L, Gu Y, Qi Z, Qiu H, et al. (2020) Immune-related lncRNA to construct novel signature and predict the immune landscape of human hepatocellular carcinoma. *Mole Ther Nucleic Acids* 22: 937-947.
19. Zhong W, Chen B, Zhong H, Huang C, Lin J, et al. (2020) Identification of 12 immune-related lncRNAs and molecular subtypes for the clear cell renal cell carcinoma based on RNA sequencing data. *Sci Repor* 10: 14422.
20. Gruss I, Twardowski JP, Cierpisz M (2019) The effects of locality and host plant on the body size of *Aeolothrips intermedius* (Thysanoptera: Aeolothripidae) in the Southwest of Poland. *Insects* 10: 266.
21. Ji P, Diederichs S, Wang W, Böing S, Metzger R, et al. (2003) MALAT-1, a novel noncoding RNA, and thymosin beta4 predict metastasis and survival in early-stage non-small cell lung cancer.
22. Brown JA, Bulkley D, Wang J, Valenstein ML, Yario TA, et al. (2014) Structural insights into the stabilization of MALAT1 noncoding RNA by a bipartite triple helix. *Nat Struct Mole Biol* 21: 633-640.
23. Brown JA, Kinzig CG, DeGregorio SJ, Steitz JA (2016) Methyltransferase-like protein 16 binds the 3'-terminal triple helix of MALAT1 long noncoding RNA. *Proc Natl Acad Sci* 113: 14013-14018.
24. Ni W, Yao S, Zhou Y, Liu Y, Huang P, et al. (2019) Long noncoding RNA GAS5 inhibits progression of colorectal cancer by interacting with and triggering YAP phosphorylation and degradation and is negatively regulated by the m6A reader YTHDF3. *Mole Cancer* 18: 143.
25. Chen M, Wei L, Law CT, Tsang FHC, Shen J, et al. (2018) RNA N6-methyladenosine methyltransferase-like 3 promotes liver cancer progression through YTHDF2-dependent posttranscriptional silencing of SOCS2. *Hepatology* 67: 2254-2270.
26. Chen Y, Peng C, Chen J, Chen D, Yang B, et al. (2019) WTAP facilitates progression of hepatocellular carcinoma via m6A-HuR-dependent epigenetic silencing of ETS1. *Mole Cancer* 18: 1-19.